

Vinson & Elkins

ATTORNEYS AT LAW

VINSON & ELKINS L.L.P.
THE WILLARD OFFICE BUILDING
1455 PENNSYLVANIA AVE., N.W.

WASHINGTON, D.C. 20004-1008

TELEPHONE (202) 639-6500

FAX (202) 639-6604

WRITER'S TELEPHONE

(202) 639-6755

EX PARTE OR LATE FILED

February 20, 1997

RECEIVED

FEB 20 1997

Federal Communications Commission
Office of Secretary

Mr. William F. Caton
Acting Secretary
Federal Communications Commission
1919 M Street, N.W.
Room 222
Washington, D.C. 20008

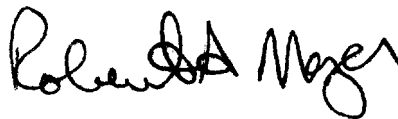
Re: IB Docket No. 96-220
Ex-Parte Presentation

Dear Mr. Caton:

Leo One USA Corporation ("Leo One USA"), by its attorneys, hereby submits for the record in the above-captioned proceeding an additional analysis of the ability of aeronautical and terrestrial meteorological satellite receivers to successfully receive signals from a meteorological satellite at elevation angles below five degrees. This analysis concludes that reception of meteorological satellite signals at elevation angles below five degrees is unreliable. Attached to this analysis is a study supporting this conclusion prepared for the Advisory Group for Aerospace Research and Development ("AGARD") by the U.S. Air Force Avionics Laboratory. Pursuant to the Commission's rules, two copies of this filing are being submitted.

If there are any questions regarding this matter, please do not hesitate to contact the undersigned counsel for Leo One USA Corporation.

Respectfully submitted,



Robert A. Mazer
Albert Shuldiner
Counsel for Leo One USA Corporation

cc: Donald Gips
Ruth Milkman
Cassandra Thomas
Harold Ng
Paula H. Ford
Julie Garcia

No. of Copies rec'd
List ABCDE

022

**Federal Communications Commission
Office of Secretary**

IB Docket No. 96-220

February 20, 1997

**AIRCRAFT RECEPTION OF 137 - 138 MHz AND 400.15 - 401 MHz METEOROLOGICAL-
SATELLITE SIGNALS SHOULD BE PROTECTED ONLY WHILE THE ASSOCIATED SATELLITE
IS LOCATED AT ELEVATION ANGLES OF FIVE DEGREES OR GREATER**

Thomas M. Sullivan

1. Introduction

The analysis of reception of Meteorological-Satellite ("MetSat") signals that was filed with the FCC by Leo One USA¹ considered typical MetSat receivers with a low-gain, hemispherical-coverage antenna operating at an unobscured site on land. These receivers are representative of Earth-based, portable, low-cost earth stations that receive transmission from NOAA and DMSP satellites. That analysis demonstrated that in light of attendant functional requirements, performance factors, and international frequency sharing criteria, MetSat earth station receivers operating at 137-138 MHz and 401.5 - 401 MHz should be protected only while the associated satellites are located at elevation angles of five (5) degrees or greater. Subsequently, questions have arisen regarding the applicability of these findings to reception of MetSat transmission by aircraft earth stations. The international performance and sharing criteria considered in the previous analysis apply equally to reception by Earth-based and airborne aircraft earth stations.² Specifically, no performance objectives or interference and sharing criteria have been developed for reception of MetSat signals by aircraft at elevation angles less than five (5) degrees. This is because functional requirements of meteorologists generally impart no need to receive MetSat transmissions at such low elevation angles, as discussed below. This notwithstanding, applicable measurements and models indicate that as for land-based earth stations, aircraft reception of MetSats below five (5) degrees elevation would not be possible as a result endemic performance limitations.

2. Functional Requirements for MetSat Reception by Aircraft

The observations made in the analysis of functional requirements for reception of MetSat signals from Earth-based receivers also apply to reception by aircraft earth stations. Specifically, the duration, geographic extent and frequency of data reception from a MetSat satellite at low elevation angles are all too small to support reliable forecasting for the corresponding distant-areas being observed by the satellite. Thus, when MetSat data are needed for these distant areas, the data are obtained either from a MetSat earth station that is proximate to the distant area (e.g., via a communication link) or from playback of data recorded by the satellite when it is observing the distant area. The fact that the MetSat satellites are visible from aircraft at lower elevation angles than from Earth-based earth stations has no bearing on the underlying requirements of meteorologists.

¹ See Comments of Leo One USA in IB Docket No. 96-220, December 20, 1996 at Appendix D.

² For the 137-138 MHz and 400.15 - 401 MHz bands, Recommendations ITU-R SA.1025-1 and SA.1026-1 specify meteorological satellite performance objectives and interference criteria for 99.9% of the time that the elevation angle is five (5) degrees or greater.

3. Performance Limitations

3.1 Department of Defense Measurements

Multipath fading levels measured for aircraft reception of VHF/UHF satellite transmissions indicate that the average fading depth at minus four (-4) degrees elevation is 4 dB and increases to 6 dB as the elevation angles is increased to five (5) degrees.³ As shown in Tables 1-3, below, the average (50%ile) values of fading for aircraft reception of 137-138 MHz and 400.15-401 MHz MetSat transmissions exceed the power margins available for fading.⁴ Even larger fade levels are exceeded for smaller but significant percentages of time. Thus, aircraft reception of MetSat signals generally is not possible at elevation angles less than five (5) degrees.

Table 1 - Comparison of Fade Margins and Average Fade Levels for Aircraft Reception of NOAA APT Transmissions (137-138 MHz)

Elevation Angle (degrees)	5	4	3	2	1	0
Fade Margin (dB)	-3.4	-3.5	-3.8	-4.1	-4.4	-4.7
Average Fade Level (dB)	6.1	5.7	5.3	5.0	4.7	4.4

Table 2 - Comparison of Fade Margins and Average Fade Levels for Aircraft Reception of LRPT Transmissions (137-138 MHz)

Elevation Angle (degrees)	5	4	3	2	1	0
Fade Margin (dB)	0.8	0.7	0.4	0.0	-0.3	-0.5
Average Fade Level (dB)	6.1	5.7	5.3	5.0	4.7	4.4

³ "Airborne Measurements of Electromagnetic Wave Reflections from Land and Sea Water," Allen L. Johnson, U.S. Air Force Avionics Laboratory, Advisory Group for Aerospace Research & Development, Conference Proceedings No. 269. See Figures 7, 14, and 18.

⁴ The fade levels presented in Tables 1-3 are average fading depths given in the reference of n.3, *infra*, for an aircraft at 30,000 feet and reception at 300 MHz (circular polarization). Frequency sensitivity of fading between 137-138 MHz and 400.15-401 MHz was found to be less than 1 dB in the analysis of Earth-based reception (n.1, *infra*). The fade margin presented in Tables 1-3 are derived from the link power budgets presented in the analysis of earth-based MetSat earth stations (n.1). Specifically, the fade margins are the sum of entries in Tables 1a, 1b, and 2 of the preceding analysis for Surface Multipath, Refractive spreading and Power margin.

Table 3 - Comparison of Fade Margins and Average Fade Levels for Aircraft Reception of DMSP Transmissions (400.15-401 MHz)

Elevation Angle (degrees)	5	4	3	2	1	0
Fade Margin (dB)	2.2	2.1	1.8	1.4	1.2	0.9
Average Fade Level (dB)	6.1	5.7	5.3	5.0	4.7	4.4

3.2 ITU-R Models of Propagation Impairments

Models for propagation impairments have been developed by the ITU-R for aeronautical earth station reception only near 1.5 GHz and at elevation angles exceeding three degrees.⁵ However, the measurements discussed above corroborate the form of the ITU-R multipath model that was applied in the analysis of reception by land-based earth stations that demonstrated that the 80%ile multipath fading (and average refractive spreading) losses exceeded the available fade margins at low elevation angles. Based on the sensitivity manifest in the ITU-R multipath and refractive spreading models to varying frequency and antenna height as well as comparison of models for aircraft and Earth-based reception near 1.5 GHz,⁶ the propagation impairments occurring with aircraft reception will differ from those with Earth-based reception in the following respects:

- (1) The refractive spreading loss experienced by airborne aircraft earth stations will be less in the range of zero-to-five degrees elevation, but will be comparable (i.e., up to about 2.7 dB) at elevation angles less than zero degrees (i.e., at positive depression angles) due to the signal path's transiting of atmosphere having a high index of refraction.
- (2) The correlation bandwidth and Doppler spread experienced during aircraft reception generally impose substantially greater degradation to aircraft reception. The correlation bandwidth for an aircraft at high altitude is less than 40 kHz; thus, receiver equalization generally is needed to receive the wider bandwidth signals of LRPT at 137-138 MHz and DMSP at 400 MHz to limit the degradation to aircraft reception.

⁵ ITU-R Recommendation 682-1, "Propagation Data Required for the Design of Earth-Space Aeronautical Mobile Telecommunication Systems."

⁶ The sensitivity of propagation impairment models to varying frequency and antenna height and comparisons of the impairments encountered with reception by aircraft and Earth-based earth stations are based on the information in ITU-R Recommendations 682-1 (n. 5, *infra*) and 681-1 ("Propagation Data Required for the Design of Earth-Space Land Mobile Telecommunication Systems"); Reports 1169 ("Sea Surface Multipath Effects in the Aeronautical Mobile-Satellite Service"), 1008-1 (used in the analysis of Earth-based MetSat earth stations), and 925-1 ("Factors Affecting the Choice of Antennas for Mobile Stations of the Land Mobile-Satellite Service"), and the ITU-R Handbook on Radiometeorology (1996).

(3) The multipath losses experienced by aircraft earth stations generally will be significantly greater than those experienced by Earth-based earth stations for a given percentage of time. The fading statistics are dependent on the location of the receiver antenna on the aircraft fuselage. If mounted atop a large fuselage in a manner that obstructs degrading surface multipath signals, then the fuselage also would obstruct the signal from the satellite when it is at low angles of elevation. If otherwise mounted to afford unobstructed view of the MetSat satellite when it is at low elevation angles, which is typical of aircraft antenna installations, then the full brunt of the surface multipath signals will be received and compounded by multipath signals from the fuselage itself.⁷

In sum, the theoretical models indicate that the net propagation impairment to reception of MetSat transmissions by aircraft at low elevation angles generally is more severe than that experienced by Earth-based receivers. Thus, it is concluded that reception of MetSat signals at elevation angles below five degrees on aircraft is at least as unreliable as reception by Earth based terminals.

⁷ The reference cited in n.x presents measured aircraft antenna "illumination factors" (i.e., ratio of antenna gain levels towards the area of Earth reflection and toward the satellite), which demonstrate that typical aircraft antennas (blade or crossed-dipole) operating at 30,000 feet altitude have illumination factors of greater than -1 dB at zero (0) degrees elevation or less. Interpolation of values averaged over all aircraft bearings relative to the satellite yields an illumination factor of -1.2 dB at five (5) degrees elevation. This means that the aircraft fuselage typically provides no substantial shielding of the degrading surface multipath signals at low elevation angles.

FROM: ALBERTA POWER CORP. TO: THE SHAREHOLDERS

TERRAIN PROFILES AND CONTOURS IN ELECTROMAGNETIC WAVE PROPAGATION

NORTH ATLANTIC TREATY ORGANIZATION



AIRBORNE MEASUREMENTS OF ELECTROMAGNETIC WAVE REFLECTIONS FROM LAND AND SEA WATER

Allen L. Johnson
U. S. Air Force Avionics Laboratory
Wright-Patterson AFB, Ohio

SUMMARY

Multipath fading caused by terrain reflections can disrupt an airborne communication or navigation system. The severity of the multipath is dependent upon the antenna illumination factor, surface reflection coefficient, and the divergence of the reflected signal. Airborne measurements have verified that severe multipath is regularly encountered over water when the aircraft is communicating with a satellite at a low elevation angle. Techniques which can reduce the multipath fading effect include the use of directive antennas, circular polarization and diversity techniques.

1. INTRODUCTION

The reflection of electromagnetic waves from the terrain can cause interference in the form of multipath fading, which can severely disrupt an airborne communication or navigation system. The basic problem explored in this paper is the development of the theoretical and measured multipath fading characteristics of a satellite-to-aircraft communication/navigation system and suggested techniques for improving system performance.

2. MULTIPATH MODEL

The multipath model which is proposed consists of a direct component and two reflective components, a specular and a diffuse, Figure 1. The severity of the effect of multipath fading is dependent upon the antenna pattern, the reflection coefficient, and the curvature of the reflecting surface. The depth of multipath fading is given by (Franklin, S. B., 1971):

$$\text{Fade depth in db} = 20 \log (1 - K^2 R/D)$$

where K^2 is the antenna illumination factor (ratio of antenna gain in direction of reflection to gain in direction of direct path); R is the reflection coefficient of the reflecting surface; and D is the divergence factor for the spreading from the curved earth.

2.1 Antenna Illumination Factor

The antenna pattern, or antenna illumination factor, has a major influence on the multipath severity. Three types of antennas are illustrated in Figure 2. The first is a blade type antenna which has a horizon coverage pattern. The horizon coverage pattern tends to illuminate the reflecting surface and generally results in a large illumination factor.

The antenna illumination factor is dependent upon the azimuth direction. Any real antenna mounted on an aircraft has nulls and peaks in its pattern, and the gain toward the satellite or toward the reflecting surface varies with the aircraft heading. The average illumination factor, K^2 , from a measured blade antenna pattern on an aircraft is given in Table I. A range of K^2 for the best and worst case aircraft directions is given in Table II.

The overhead antenna pattern characteristics of a cross-dipole antenna give considerable protection to the multipath reflective component when the satellite is at a high elevation angle. This discrimination results in a low antenna illumination factor, Table I.

A third antenna type is a directive antenna primarily used at the microwave frequencies. The directive antenna, again, gives good protection against the reflected signal unless the satellite is right on the horizon, Table I.

TABLE I: Antenna Illumination Factor (K^2) for Various Antennas*
(For Aircraft at 30,000 Ft.)

ELEVATION: ANGLE	AVERAGE HORIZON ANTENNA	AVERAGE OMNI ANTENNA	AVERAGE OVERHEAD ANTENNA	AVERAGE DIRECTIONAL ANTENNA
90°	.18	.10	.026	.003
80°	.14	.10	.026	.003
70°	.14	.10	.032	.003
60°	.14	.10	.032	.003
50°	.14	.14	.032	.003
40°	.18	.18	.04	.01
30°	.22	.32	.05	.02
20°	.50	.56	.08	.03
10°	.71	.71	.20	.10
0°	.94	.94	.89	.16
-3°	1.00	1.00	1.00	1.00

*from Burnside, W. D. et al 1973
Clanton, S., 1974
Maroth, V., 1963

TABLE II: Antenna Illumination Factor Variances (K^2)*
(For Aircraft at 30,000 ft.)
Typical Horizon Coverage, Antenna

ELEVATION ANGLE	MINIMUM K^2	AVERAGE K^2	MAXIMUM K^2
90°	.10	.18	1.00
80°	.10	.14	.79
70°	.03	.14	.56
60°	.03	.14	.31
50°	.03	.14	.55
40°	.03	.18	.56
30°	.03	.22	.79
20°	.03	.50	.79
10°	.10	.71	.89
0°	.89	.94	1.00
-3°	1.00	1.00	1.00

*from Clanton, S., 1974

2.2 Reflection Coefficient

The reflection coefficient used in the preceding equation is a combination of the basic reflection coefficient of the surface multiplied by the specular, or diffuse, reflection coefficient. The basic reflection coefficient is dependent upon the type of reflecting surface, the polarization of the reflected wave, the elevation angle of the reflection and frequency.

For a horizontally polarized incident wave, the reflection coefficient is given by (Reed and Russell, 1964):

$$R_h = \frac{\sin \psi - \sqrt{n^2 - \cos^2 \psi}}{\sin \psi + \sqrt{n^2 - \cos^2 \psi}}$$

where n^2 is a complex reflectivity factor = $\epsilon_r - j \frac{18000 \sigma}{f_c}$

ψ is the grazing angle shown in Figure 3

ϵ_r is the relative dielectric constant

σ is the conductivity in mhos/meter

f_c is the carrier frequency in MHz

Neither the amplitude nor phase of the horizontal reflection coefficient is very sensitive to the physical surface constants nor frequency, Figure 4. Typical values of the physical constants for various types surfaces are given in Table III.

TABLE III: Physical Properties of Various Reflecting Surfaces*

SURFACE TYPE	PERMEABILITY μ	DIELECTRIC ϵ_r	CONDUCTIVITY σ
Free space	$1.257 \times 10^{-6} = \mu_v$ Henry/meter	$8.855 \times 10^{-12} = \epsilon_v$ Farad/meter	mho/meter
Distilled Water		78	1×10^{-6}
Fresh water		80	8×10^{-3}
Sea water		80	5
Ice (fresh water)		3	2×10^{-6}
Dry, sandy, flat coastal land (dry earth)		5	1×10^{-6}
Marshy, forested, flat land (wet earth)		30	1×10^{-2}
Farmland -- low hills		15	1×10^{-2}
Pastoral land, medium hills		13	5×10^{-3}
Rocky land, steep hills		10	2×10^{-3}
Mountainous		5	1×10^{-3}
City, residential area		5	2×10^{-3}
City, industrial area		3	1×10^{-1}

*from Kerr, D. E., 1951
Reed and Russell, 1964

When there is water, snow or ice over another surface such as land, the depth of penetration of the electromagnetic wave determines whether the top surface or a combination of the top and underlying surface determine the physical constants. The depth of penetration is given by (Jordan, E. C., 1955):

$$\delta = \frac{\mu \epsilon \left[\left(1 + \frac{\sigma^2}{\omega^2 \epsilon^2} \right)^{1/2} - 1 \right]}{\omega}$$

where: δ = depth of penetration

μ = permeability in Henry/meter

ϵ = dielectric constant in Farad/meter

σ = conductivity in mhos/meter

$\omega = 2\pi f_c$ in Hertz

f_c = carrier frequency in Hertz

The depth of penetration for several surfaces at 300 MHz is given in Table IV.

TABLE IV: Depth of Penetration
(For 300 MHz)

Sea Water	0.015 meters
Fresh water	5.93 meters
Ice	45.93 meters
Average land	2.06 meters

For a vertically polarized incident wave, the reflection coefficient is given by (Reed and Russell, 1964):

$$R_v = \frac{n^2 \sin \psi - \sqrt{n^2 - \cos^2 \psi}}{n^2 \sin \psi + \sqrt{n^2 - \cos^2 \psi}}$$

The amplitude of the vertical reflection coefficient goes through a minimum at a grazing angle (called the Brewster angle) which is dependent on the physical surface constants and frequency. Two examples are shown in Figure 4. The phase goes through a 180° reversal around the point of minimum amplitude.

For a circularly polarized incident wave, the reflection coefficient is given by (Chinnick, J. H., 1977):

$$R_{cs} = \frac{\sqrt{R_h^2 + R_v^2 + 2 R_h R_v \cos (\phi_h - \phi_v)}}{2}$$

when the direct and reflected waves have the same sense circular polarization

$$\text{and } R_{co} = \frac{\sqrt{R_h^2 + R_v^2 - 2 R_h R_v \cos (\phi_h - \phi_v)}}{2}$$

when the direct and reflected waves have opposite sense circular polarization.

The amplitude of the same sense circular reflective coefficient falls between the horizontal and vertical reflection coefficients. The amplitude of the opposite sense circular reflection coefficient starts high at large grazing angles like the horizontal reflection coefficient and goes to zero as the grazing angle decreases to zero.

The surface roughness will determine the ratio of specular to diffuse reflected energy. For a smooth surface the specular component will predominate, while for a rough surface, the diffuse scattered component predominates, Figure 5 (Beckmann and Spizzichino, 1963). For a relatively smooth surface the coherent scattering is limited to the first Fresnel Zone. However, for a very rough surface such as a rough sea, the scattering may come from a considerably larger area.

Surface roughness tends to be elevation angle dependent. Even the very rough sea appears smooth when viewed from a very low elevation angle. The relationship between surface roughness and elevation angle is shown in Table V. When the grazing angle exceeds about twice the critical angle shown in Table V, the specular component becomes insignificant and the reflection coefficient depends upon the diffuse scattering factor.

TABLE V: Maximum Angles for Specular Reflection at Different Frequencies and Sea States*

Sea State Number	Description of Sea	Wave Height (m)	Rms Height, σ_h (m)	Critical Angle, γ_{\max} (deg)			
				$\lambda=0.7$ m	$\lambda=0.23$ m	$\lambda=0.1$ m	$\lambda=0.03$ m
1	Smooth	0-0.3	0-0.065	>45	>13	>6	>1.8
2	Slight	0.3-1	0.065-0.21	12-45	4-13	1.8-6	0.5-1.8
3	Moderate	1-1.5	0.21-0.32	8-12	2.6-4	1.2-1.8	0.3-0.5
4	Rough	1.5-2.5	0.32-0.54	5-8	1.6-2.6	0.7-1.2	0.2-0.3
5	Very rough	2.5-4	0.54-0.86	3-5	1-1.6	0.4-0.7	0.12-0.2
6	High	4-6	0.86-1.3	2-3	0.7-1	0.3-0.4	0.04-0.12
7		>6	>1.3	<2	<0.7	<0.3	<0.04

*from Beckmann and Spizzichino, 1963

2.3 Divergence Factor

The divergence factor takes into consideration the convex shape of the reflecting surface.

The divergence is given by (Beckmann and Spizzichino, 1963):

$$D = \left(1 + \frac{2 d_1 d_2}{r (d_1 + d_2) \sin \psi} \right)^{-\frac{1}{2}} \left(1 + \frac{2 d_1 d_2}{r (d_1 + d_2)} \right)^{-\frac{1}{2}}$$

Refer to Figure 3 for definition of terms.

The divergence is very sensitive to the height of the receiving antenna. The divergence factors for an antenna at 100 feet, 30,000 feet, and 70,000 feet is shown in Figure 6 (Foley, et al, 1968)

2.4 Fade Rate

The multipath fade rate can be determined geometrically by calculating the rate of change of the path difference between the direct and the reflected component (Bond, F.E., 1967).

$$\text{Fade rate} = \frac{d\theta}{dt} \frac{d(\Delta d)}{d\theta} \frac{f_c}{c}$$

(See Figure 3 for definition of terms).

Where θ = great circle angle between aircraft and satellite

$$\Delta d = d_1 + d_2 - d$$

$$f_c = \text{carrier frequency}$$

$$c = \text{speed of light}$$

$$d = [(r + h_1)^2 + (r + h_2)^2 - 2(r + h_1)(r + h_2) \cos \theta]^{\frac{1}{2}}$$

$$d_1 = [r^2 + (r + h_1)^2 - 2r(r + h_1) \cos \beta]^{\frac{1}{2}}$$

$$d_2 = [r^2 + (r + h_2)^2 - 2r(r + h_2) \cos \delta]^{\frac{1}{2}}$$

$$\theta = \beta + \delta$$

$$\cos \beta = \frac{r}{r + h_1} \left(w + [w^2 + \left(\frac{r + h_1}{r} \right)^2 - w \left(\frac{r + h_1}{r} \right)^2 - w]^{\frac{1}{2}} \right)$$

where

$$w = \frac{(r + h_2)^2 \sin^2 \delta}{(r + h_2)^2 + r^2 - 2r(r + h_2) \cos \delta}$$

These equations predict the fade rates shown in Figure 7. Measurement of the power spectral density of the signal shown in the top of Figure 7 is plotted in Figure 8 (Johnson, et al, 1979). While the diffuse power spectral density decreases at approximately f^{-2} , a very strong specular component can be seen at approximately .75 Hz. The autocorrelation function of this same signal shows a repetitive correlation with a spacing of approximately 1.3 seconds, Figure 9.

3. MEASUREMENT TECHNIQUES

3.1 Psuedo-Random Sequence

One of the measurement techniques used to separate the direct and reflected signal component is the use of psuedo-random (PRN) sequence and correlation technique. One PRN system which has been tested utilized a 127 bit direct psuedo-random sequence transmitted through the satellite (Prettle, et al, 1977). At the receiving terminal the matching 127 bit psuedo-random sequence was correlated with the received signal and

between the direct and the reflected correlation indicates the amplitude difference of the direct and reflected signals. The time difference indicates differential path delay.

The results of the PRN correlation technique with the satellite at a high elevation angle are shown in Figure 11 for an overhead type antenna (Johnson, A. L., 1978-1). The reflected signal is delayed approximately 50 microseconds and is approximately 20 db lower in amplitude than the direct signal. The results in Figure 12 are for a horizon coverage antenna at a satellite elevation angle of 24°. Here the reflected signal is only approximately 1 db below the direct signal. A rather long trail of diffuse energy is evident with delays up to 15 microseconds later than the specular component. The energy reflected from ice, Figure 13, is approximately 5 to 10 db below the direct signal. The reflections from land, even at relatively low elevation angles (Figure 14) are down significantly from the water reflected multipath.

3.2 Directive Antennas

Another technique which provides information on the reflected component is the use of a directive, bottom-mounted antenna and a separate antenna mounted on top of the aircraft (Prettie, C. W., 1977). This technique allows the measurement of the direct and reflected components for medium to high elevation angles, as shown in Figure 15. Over water the bottom antenna yielded a strong reflected signal at high elevation angles with the average reflected energy approximately 6 db less than the direct received energy (Johnson, A. L., 1979). The bottom received signal, Figure 16, appears noise-like with fade rates of 10 to 100 Hz and a peak-to-null amplitude of 10 to 15 db. Over land, at a high elevation angle, the bottom antenna yielded a less consistent reflected signal, Figure 17. The average signal energy was approximately 10 db less than the direct signal.

4. IMPROVEMENT FACTORS

4.1 Antenna Polarization

The fact that the reflection coefficient is dependent upon antenna or signal polarization leads to the obvious conclusion that different signal polarizations will experience different multipath fading depths. Experimental observations have confirmed the predicted results. Measurements of the signal received from a satellite utilizing a linear antenna polarization showed that the multipath fading depth increased sharply as the elevation angle decreased, Figure 18. Multipath fade depths of greater than 20 db were experienced at very low elevation angles (Jorden, K. L., 1969).

However, satellites which employ circular polarization provide considerable protection against low angle multipath fading. Extensive measurements are summarized in Figure 18 showing that the multipath fading tends to peak up at a moderately low elevation angle with the fade depth seldom exceeding 10 or 12 db (Johnson, A. L., 1974). As the elevation angle decreased, the fade depth decreased to approximately 5 db.

4.2 Antenna Directivity

If a directive aircraft antenna can be used to minimize the illumination of the reflecting surface, the multipath fade depth can be reduced significantly. As discussed in Section 2.1, antenna directivity is the largest multipath fade factor under the system designer's control.

4.3 Diversity Techniques

Due to the multipath geometry, the multipath fading is very frequency selective. As a result, frequency diversity techniques work extremely well to overcome the multipath fading. The results of a triple frequency diversity scheme are shown in Figure 19 (Johnson, A. L., 1968). The maximum frequency separation from Frequency 1 to Frequency 6 is 300 KHz. The elevation angle at which this multipath occurred was approximately 8°. From Figure 19 it can be seen that when Frequency 1 is in a fade, Frequency 6 is at its multipath peak. The utilization of a diversity combiner can virtually eliminate the effect of this type of multipath fading.

Another example of frequency diversity is rapid frequency hopping of a signal where the hopping rate is greater than the data rate (Johnson, A. L., 1972). Figure 20 shows the received signal level of an unhopped and a fast-hopped signal. Combining the multiple frequency hopped chips into a single data bit significantly reduces the effect of the multipath fading period.

Space, or antenna diversity, can significantly reduce the multipath fading if the antennas are spaced far enough apart to decorrelate the fading. Vertical spacing of approximately 5 to 10 wavelengths is usually sufficient to decorrelate the fading. Horizontal spacing of 50 to 100 wavelengths is needed to provide similar decorrelation.

Time diversity techniques also improve multipath fading performance. The use of error correction coding can provide the needed time diversity. Usually interleaving of data bits is required to break up the burst errors which multipath fading produce. Error correction coder/decoders can only effectively correct random error patterns.

5.0 UNEXPECTED MULTIPATH RESULTS

5.1 Coastal Multipath

An unexpected result of the bottom antenna test described in Section 3.2 was the discovery of a strong, specular reflective component as the aircraft passed over a coastal area. This effect was noted as the aircraft flew in the vicinity of the Gulf of Mexico at a high elevation angle to the satellite. An irregular, noise-like signal was experienced as the aircraft flew over Texas, Figure 21. As the aircraft approached the coast of Texas, a specular reflection was received for approximately one minute. The aircraft then flew

of 10 to 15 miles. This specular component is not peculiar to the Texas coast, but has been recorded along the coast of Louisiana, Virginia, Canada, Greenland, Mexico, Central America and Hudson Bay (Johnson, et al, 1977 and 1979). The strength of the specular reflection is so great that its effect is visible on an upward-looking antenna, Figure 22. The upward antenna has a discrimination factor of approximately 30 db between the direct and reflected signal. The ringing type multipath shown in Figure 22 was recorded as the aircraft passed over the coast of Louisiana (Johnson, A. L., 1978-2). The 2 db of multipath is the result of a reflected signal which is down approximately 14 db below the direct signal.

6. CONCLUSION

Test results have confirmed that severe multipath fading can be experienced when the aircraft is communicating with a satellite at low elevation angles. Over water a deep, continuous multipath is usually experienced, while over land, a sporadic multipath is usually encountered. Techniques which can significantly reduce the multipath fading include antenna discrimination, use of circular polarization and frequency diversity.

REFERENCES

- Beckmann, P. and Spizzichino, A., 1963, The Scattering of Electromagnetic Waves from Rough Surfaces, MacMillan Co., New York, 1963.
- Bond, F. E., 1967, Precise Results for Differential Delay and Fading Rate For Aircraft/Satellite Link (Draft), Aerospace Corp.; Los Angeles, Calif.; 30 Oct 67.
- Burnside, W. D. and Marhefka, R. J., Yu, C. L., 1973, Roll-Plane Analysis of On-Aircraft Antennas, IEEE Transaction on Antennas and Propagation, Vol. AP-21, #6, pp. 780-786; Nov 73.
- Chinnick, J. H., 1977, A Report On Low Angle Ocean Scatter Measurements, Communication Research Centre Report; Ottawa, Canada, 29 Aug 1977.
- Clanton, Steve, 1974, AFSCS Antenna Patterns on B52-K, Boeing Test Report T-3-1687; Renton, Wash.; 25 April 74.
- Foley, T. K., Gaumond, B. J. and Sestak, E., 1968, Experimental L-Band SST Satellite Communication/Surveillance Terminal Study, Boeing Report D6-60105-2, Vol. III; Renton, Wash.; Nov 1968.
- Franklin, Sidney B., 1973, A Brief Summary of Multipath Effects That Will Tend to Limit RPV-to-Relay Range, AFAL Tech Memo; WPAFB, Ohio, 6 Nov 73.
- Johnson, Allen L., 1968, Six-Month Report of Flight Test Results on Program 591, Air Force Avionics Laboratory; WPAFB, Ohio, 31 Jan 68.
- Johnson, Allen L., 1974, UHF Multipath Fading, Air Force Avionics Laboratory Memo for Record, WPAFB, Ohio, 9 September 1974.
- Johnson, Allen L., 1977, Test Results from June 1977 Polar Flight Test, Air Force Avionics Laboratory Tech Memo: AFAL-TM-77-57; WPAFB, Ohio; 8 Oct 1977.
- Johnson, Allen L., 1978-1, Aircraft to Satellite Multipath Test, Air Force Avionics Laboratory Tech Memo: AFAL-TM-78-5, WPAFB, Ohio, 30 January 1978.
- Johnson, Allen L., 1978-2, Dual Frequency SATCOM Atlantic Flight Test Report, Air Force Avionics Laboratory Tech Memo: AFAL-TM-78-34; WPAFB, Ohio, 25 Dec 78.
- Johnson, Allen L., 1979, UHF Multipath Test, Air Force Avionics Laboratory Tech Memo: AFAL-TM-79-2; WPAFB, Ohio, 1 March 1979.
- Johnson, Allen L., Beach, Robert C., 1977, Atlantic Flight Test, Air Force Avionics Laboratory Tech Memo: AFAL-TM-77-71; WPAFB, Ohio, 23 Dec 1977.
- Johnson, A., Swanson, R. and Beach, R., 1979, 1979 SATCOM Polar Flight Test, Air Force Avionics Laboratory Tech Memo: AFAL-TM-79-1; WPAFB, Ohio 28 Feb 79.
- Jordan, Edward C., 1955, Electromagnetic Waves and Radiating Systems, Prentice-Hall: New York, 1955.
- Jorden, Kenneth L., Jr., 1969, Multipath Characteristics in a Satellite-Aircraft Link at 230 MHz, MIT Lincoln Laboratory Report MS2605, Lexington, Mass., September 1969.
- Kerr, D. E., 1951, Propagation of Short Radio Waves, MIT Radiation Laboratory Series, Vol. 13, McGraw-Hill Book Publishers, Inc., New York, 1951.
- Maroth, V., 1963, Model Radiation Pattern Study AT-1076A Antenna on the KC135 Aircraft, Engineering Report 1610.1, Dorne & Margolin; Westbury, New York; 2 April 1963.
- Prettie, Clifford W., 1977, Test Plan for A Sea Multipath Spatial Diversity Experiment, ESL, Inc., Sunnyvale, Calif., August 1977.
- Prettie, Dr. C., Johnson, A., Marshall, Dr. J., Grizinski, T., and Swanson, R., 1977, Project Stress Satellite Communication Test Results, AFAL-TR-77-158, Air Force Avionics Laboratory, WPAFB, Ohio, July 1977.

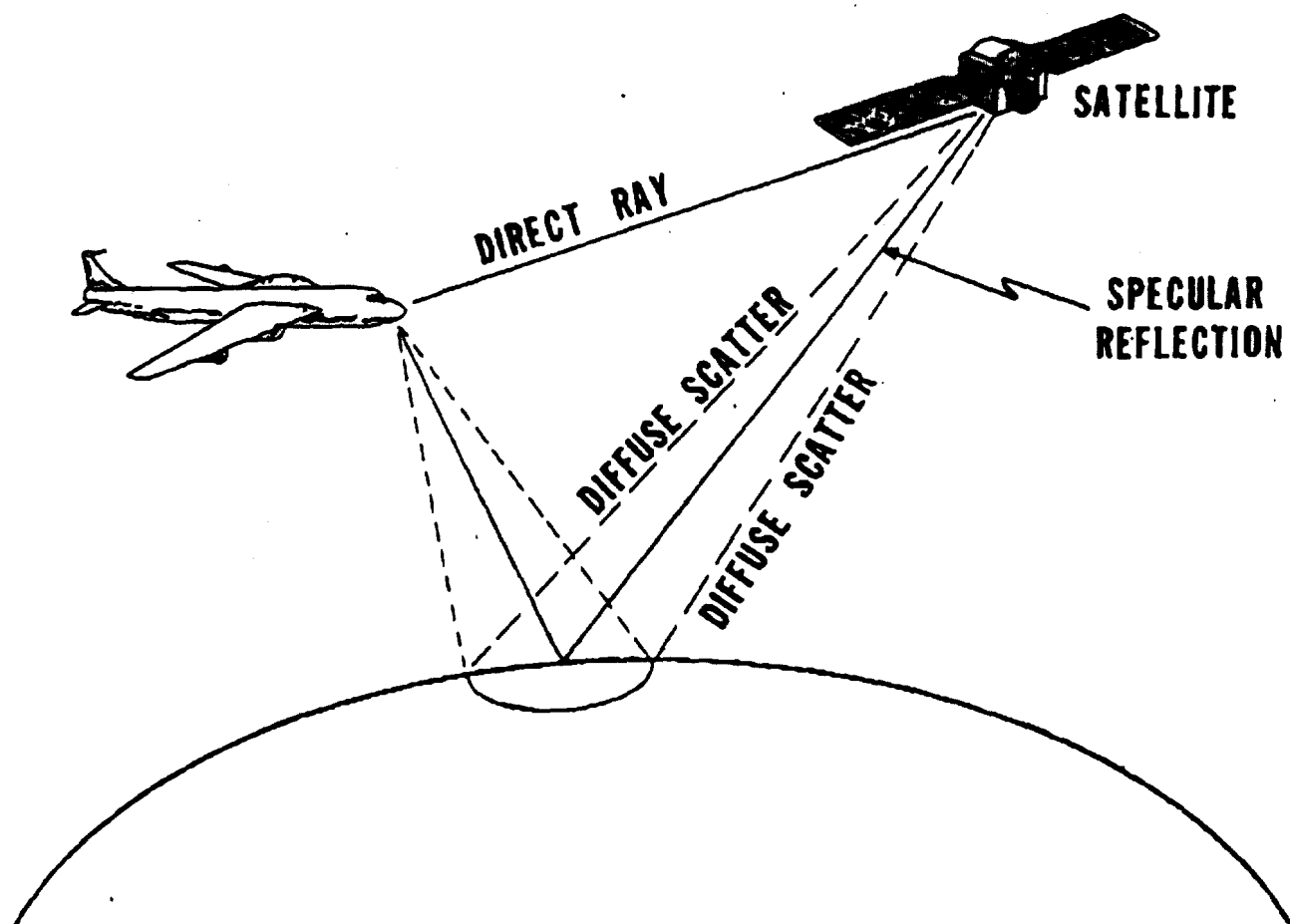


Fig.1 Multipath geometry

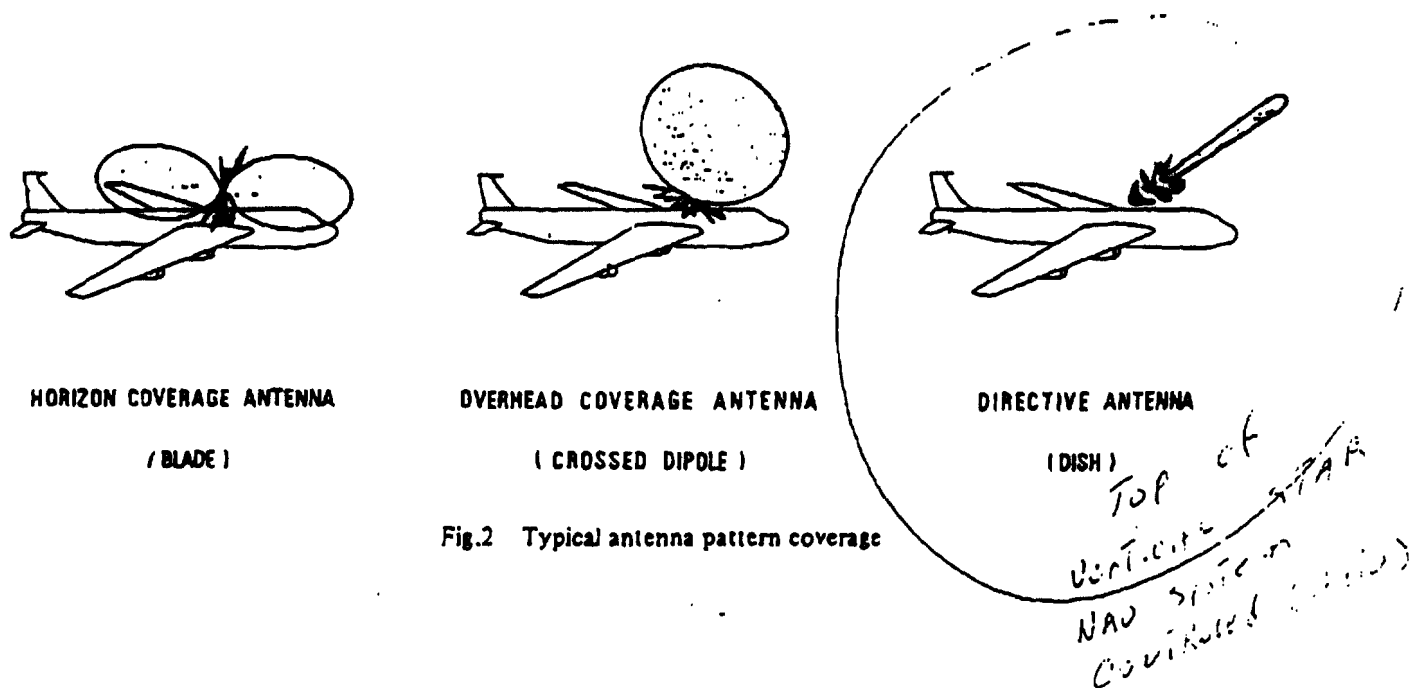


Fig.2 Typical antenna pattern coverage

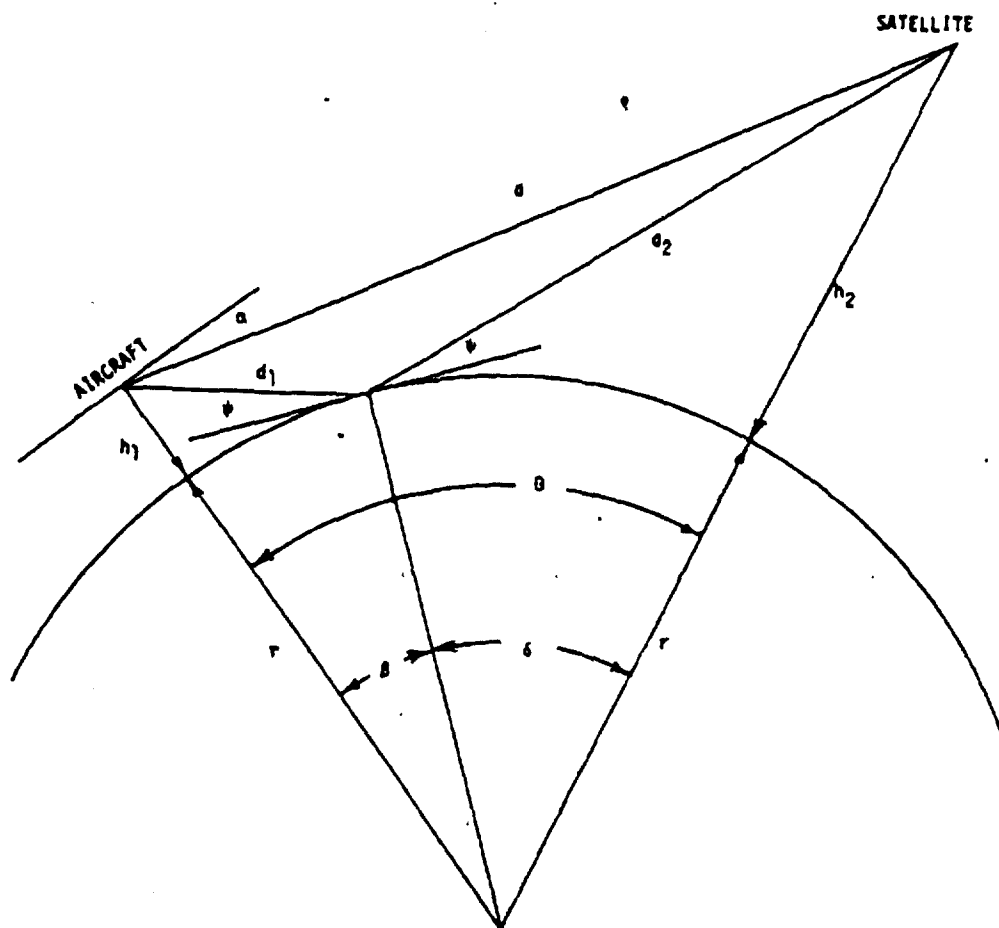
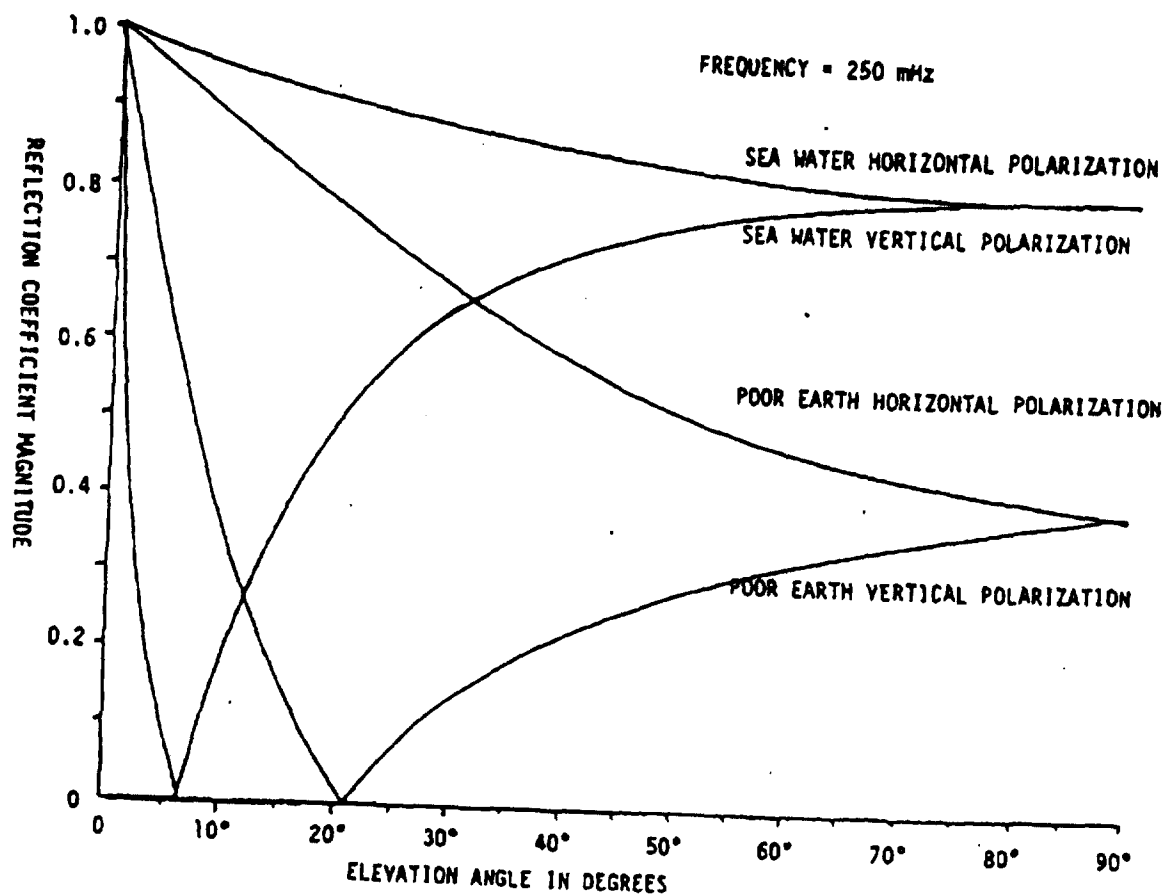


Fig.3 Multipath geometry



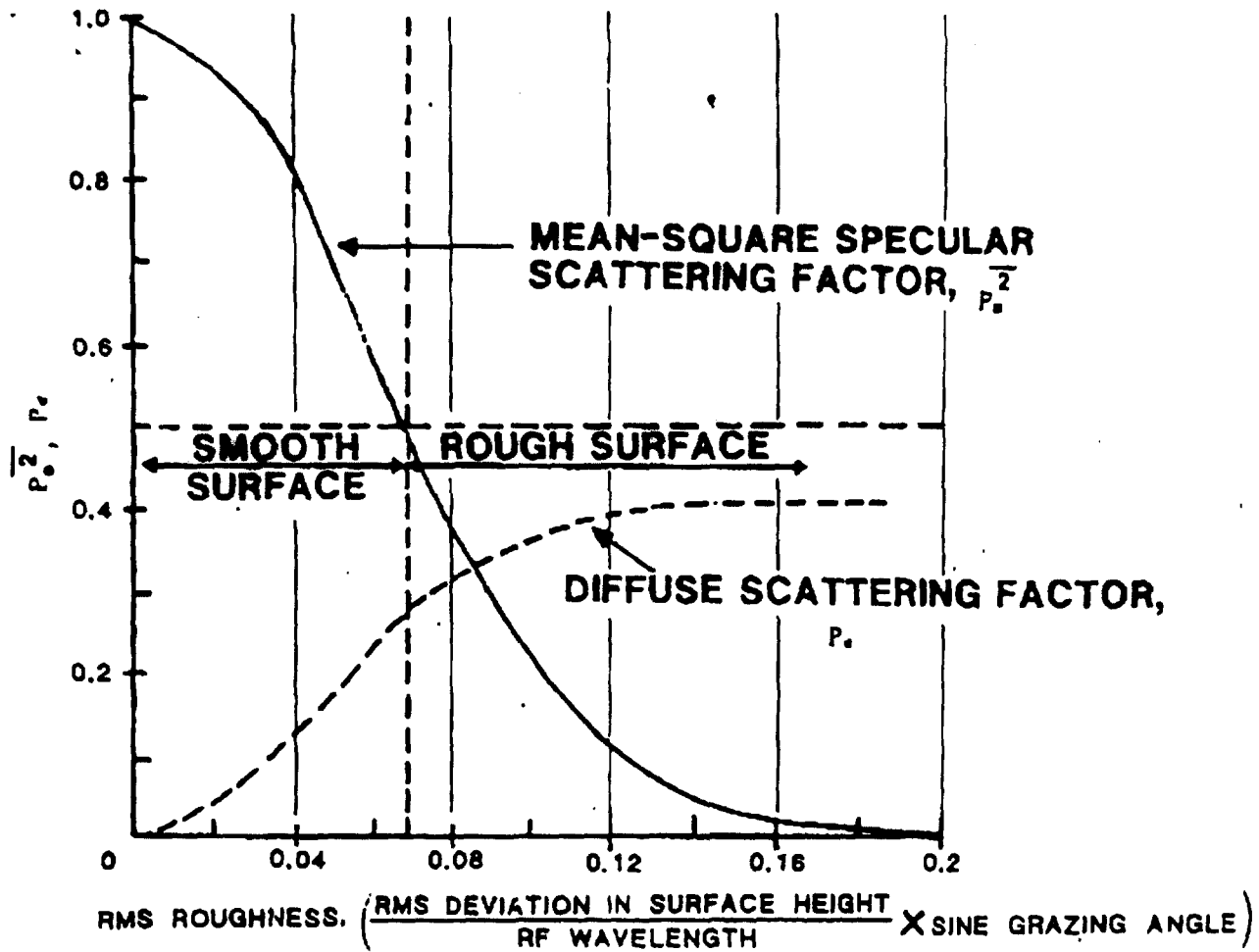
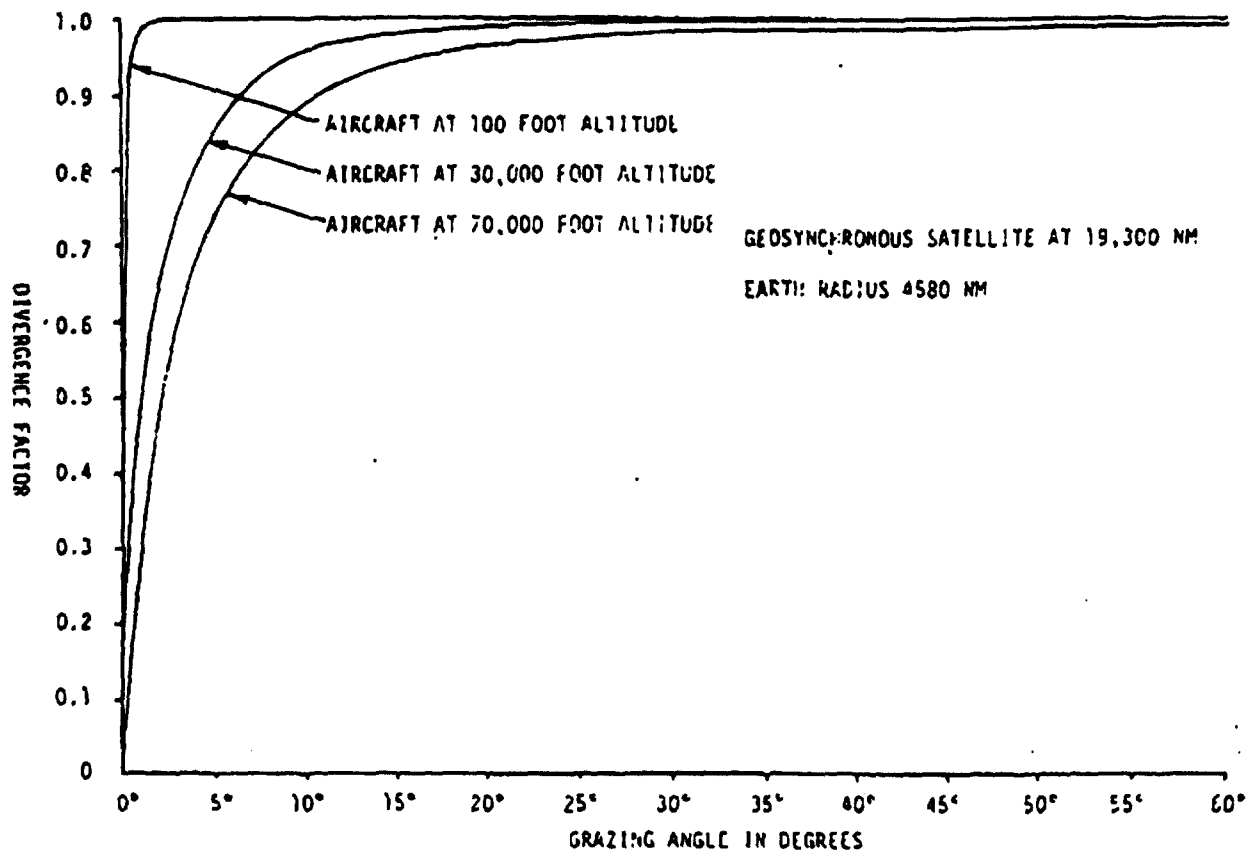


Fig.5 Scattering factors versus roughness



26 JANUARY 1979
 AIRCRAFT C-135/662
 LES 8 UHF
 TOP BLADE ANTENNA
 POLAR CAP

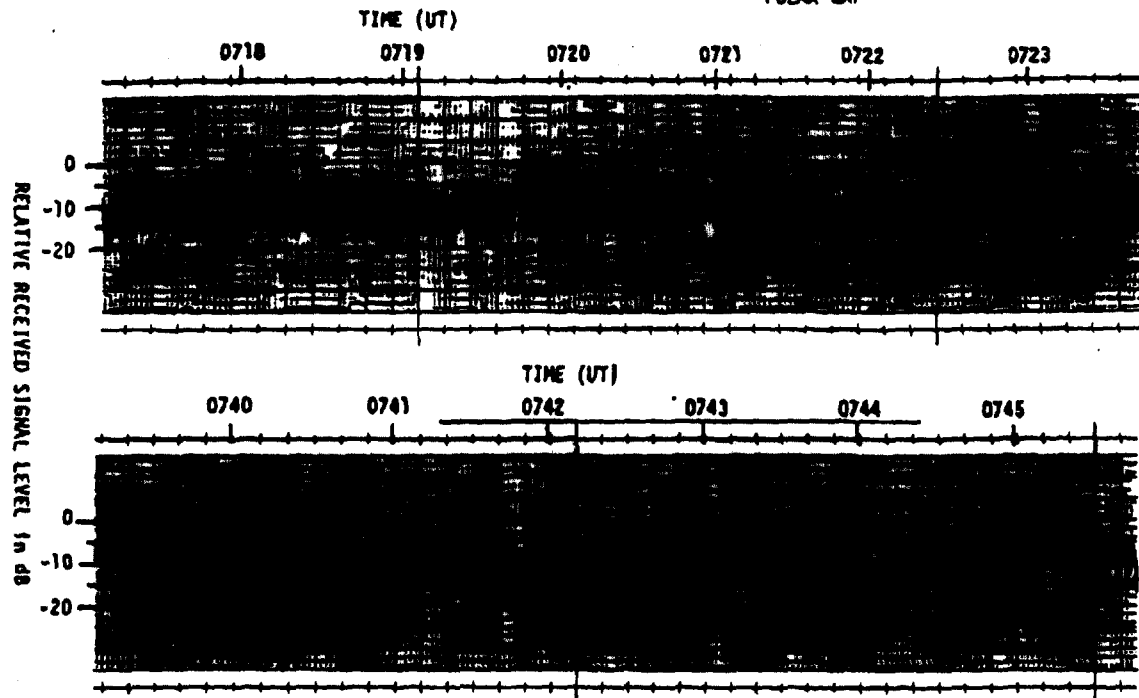
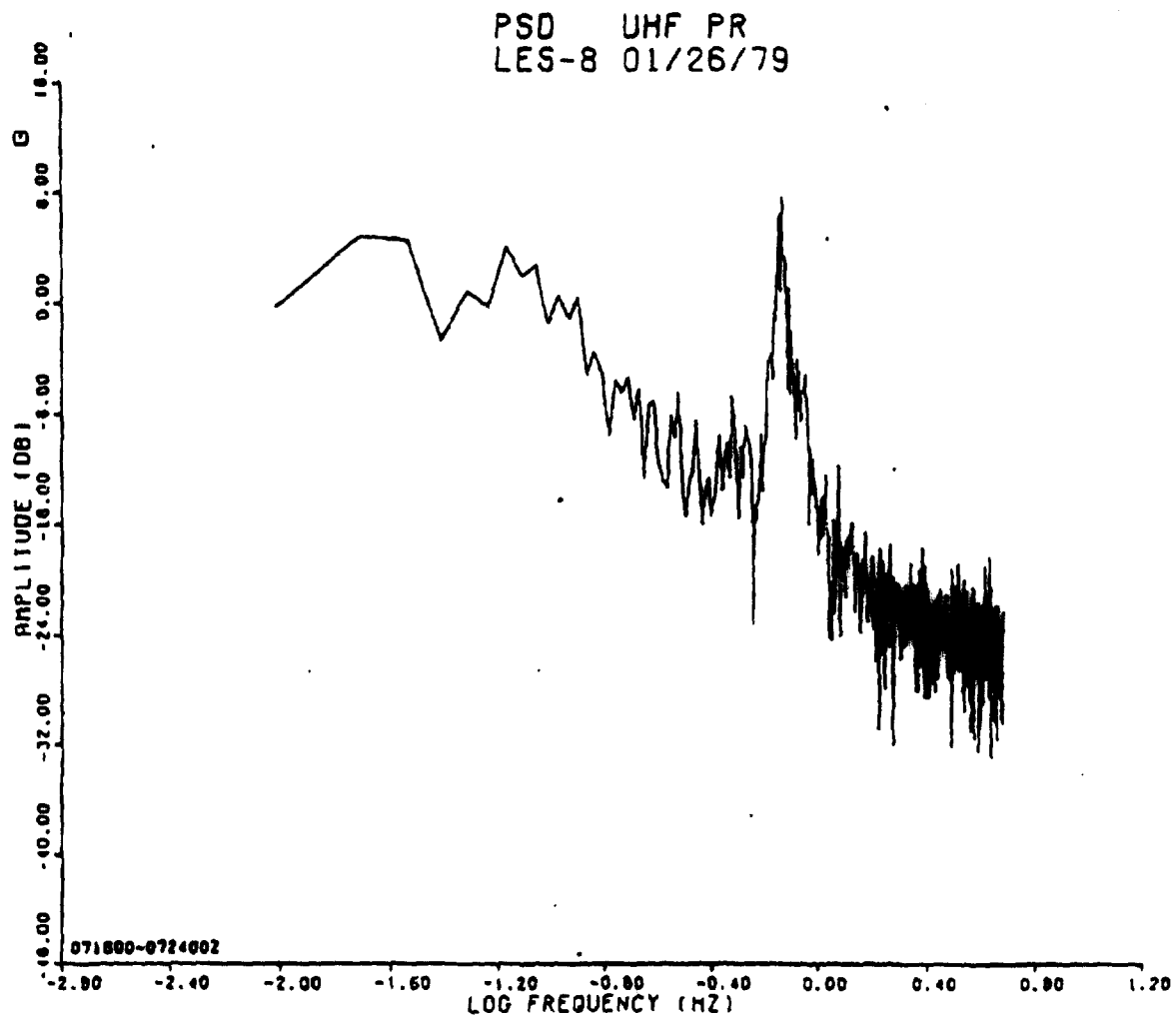


Fig.7 Example of low elevation angle UHF multipath fading



UHF PR
LES-8, 01/25/79

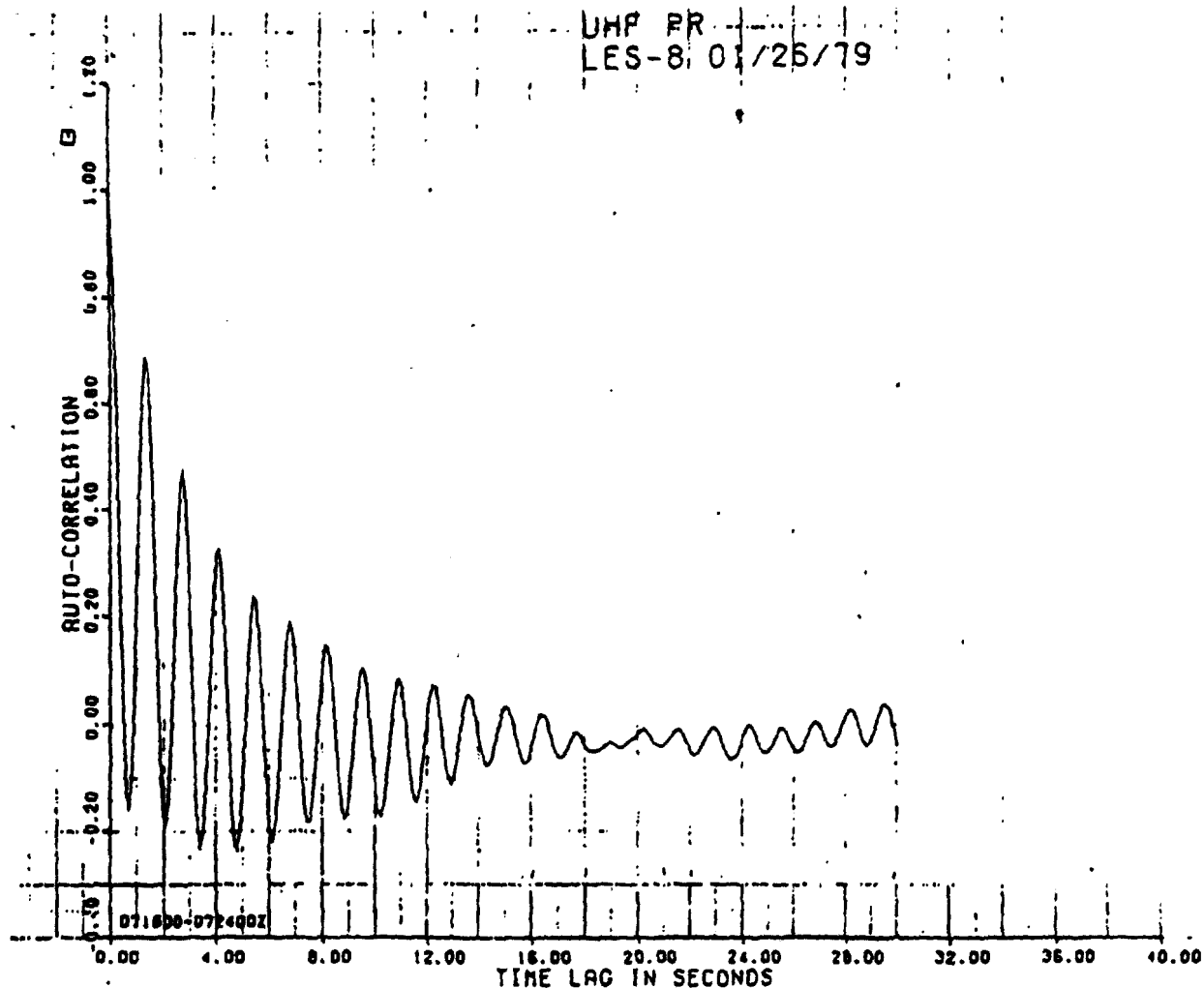
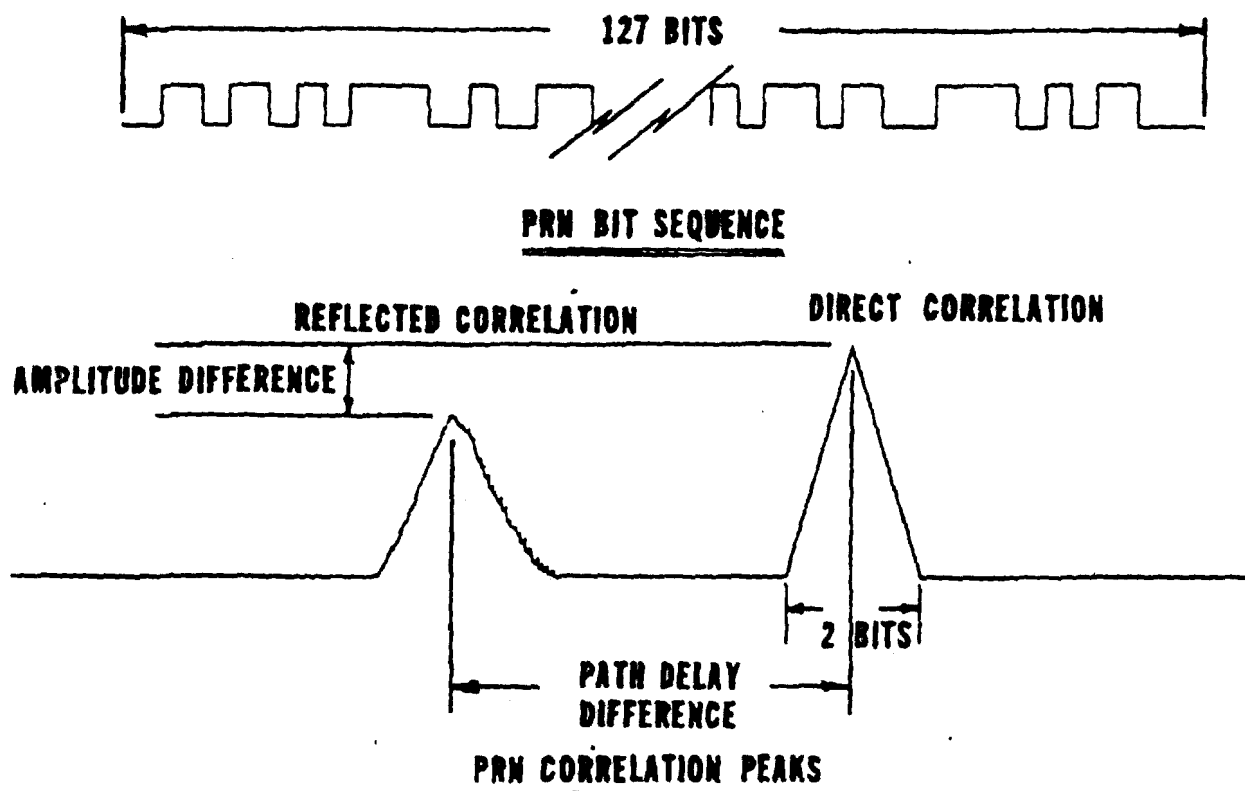


Fig.9 Autocorrelation of multipath signal



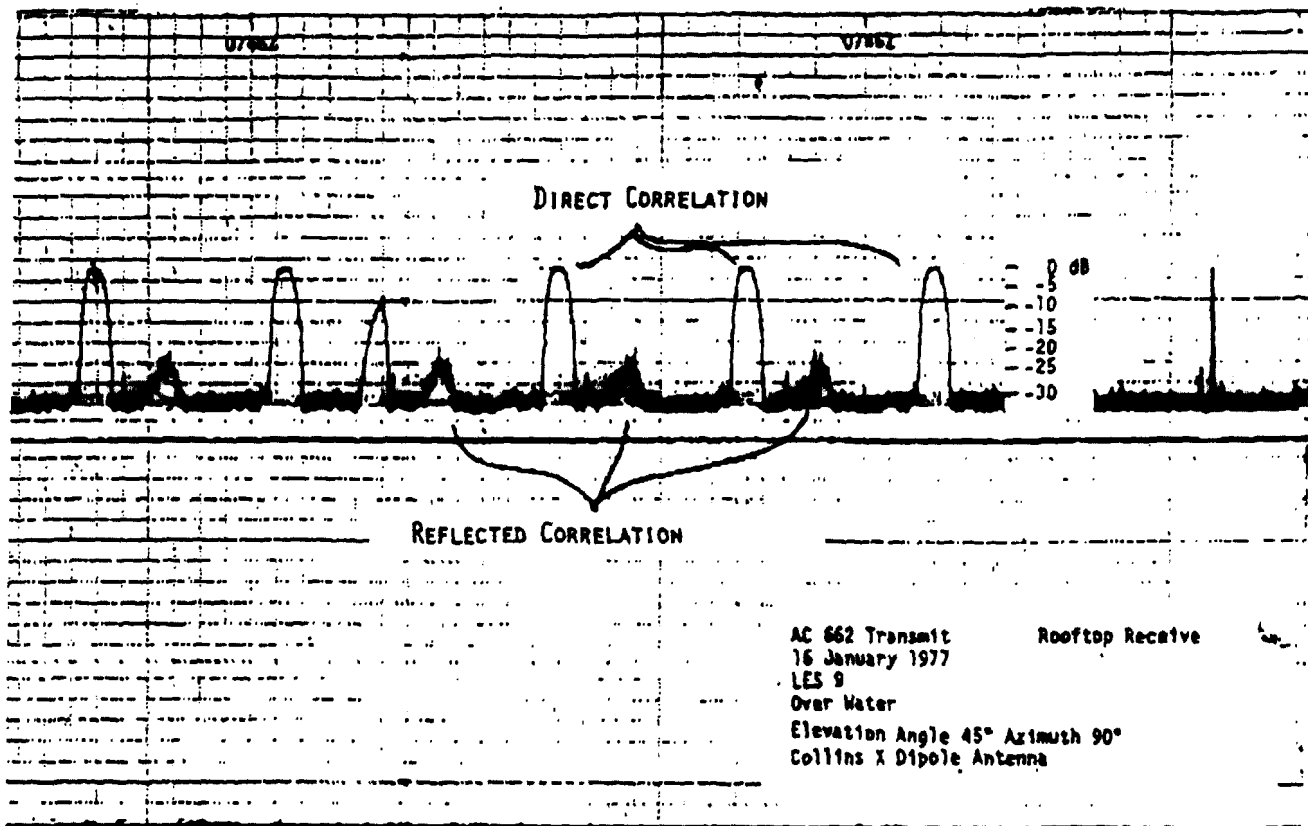


Fig.11 Results of PRN correlation with overhead antenna

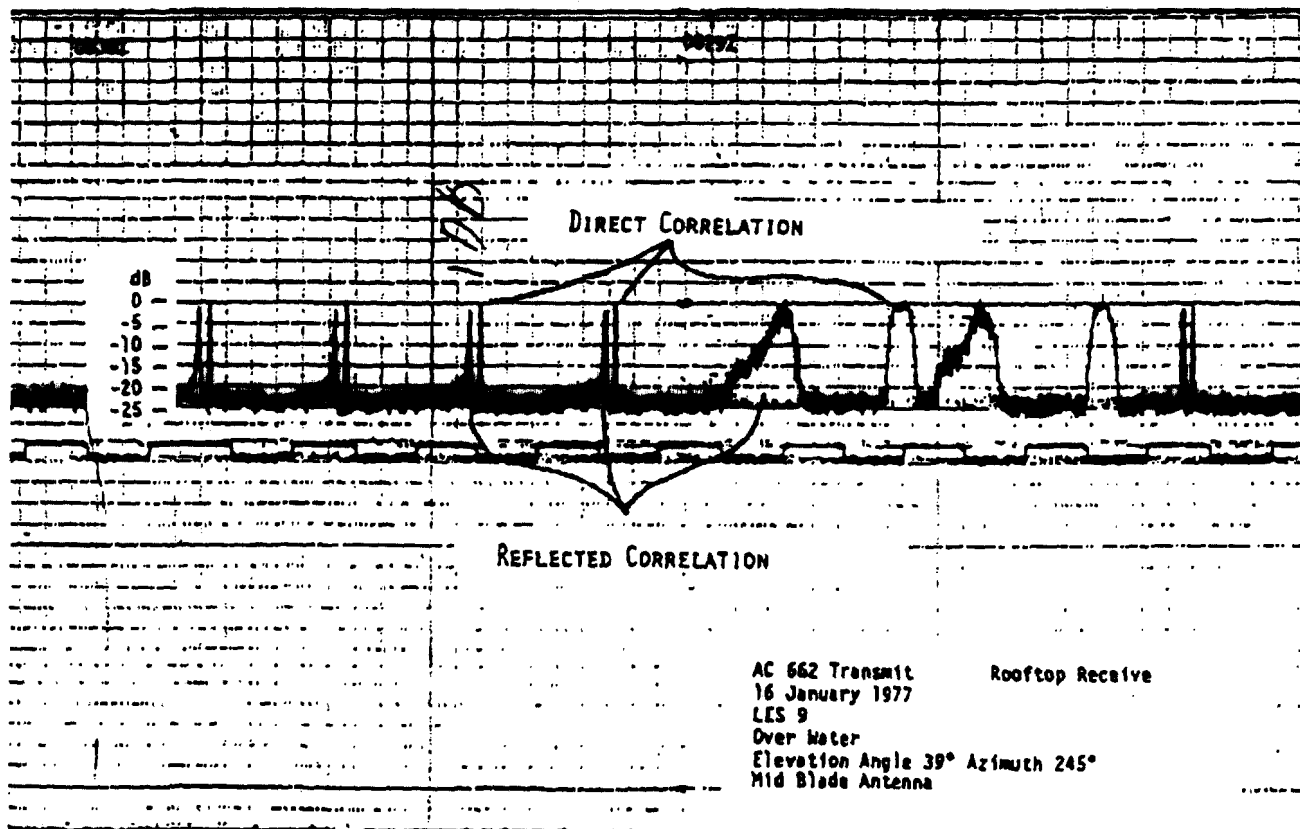


Fig.12 Results of PRN correlation with horizon antenna over water

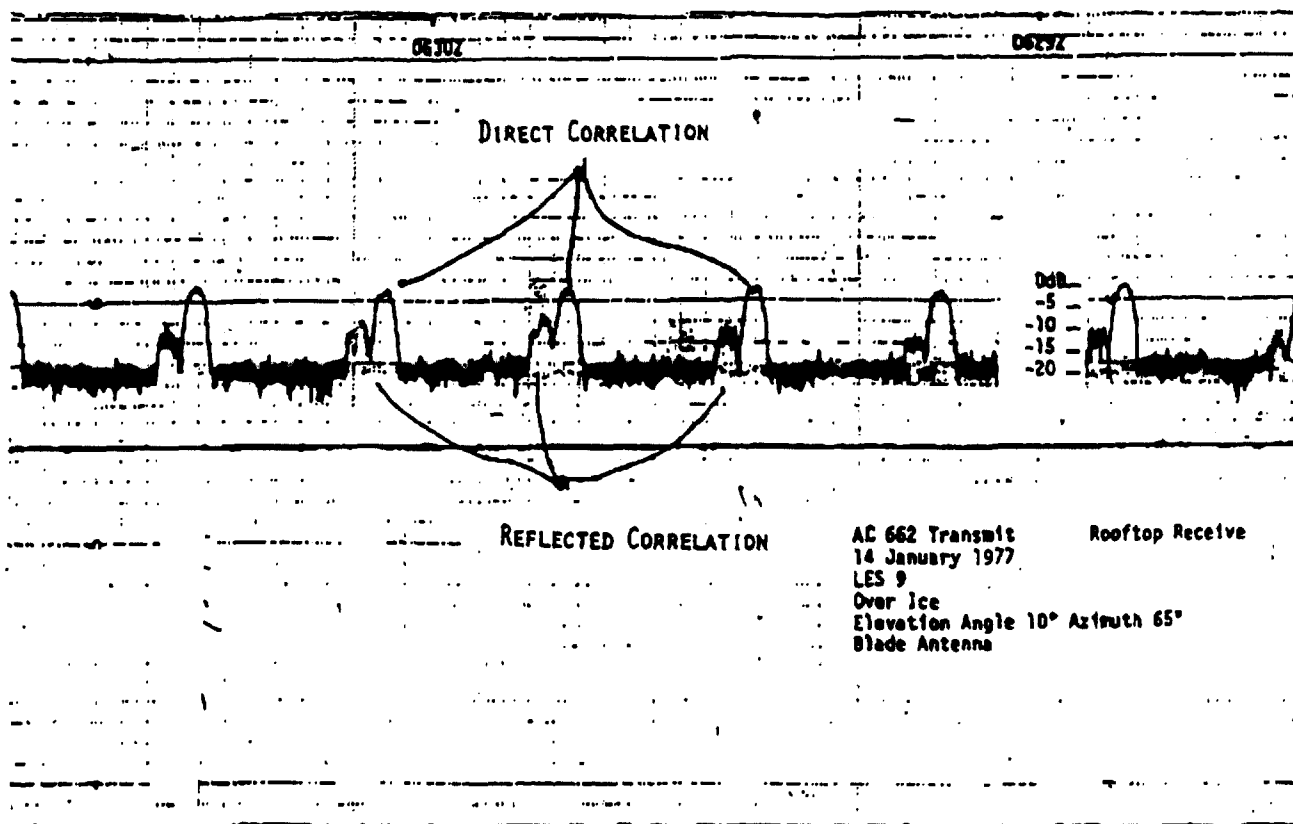


Fig.13 Results of PRN correlation with horizon antenna over ice

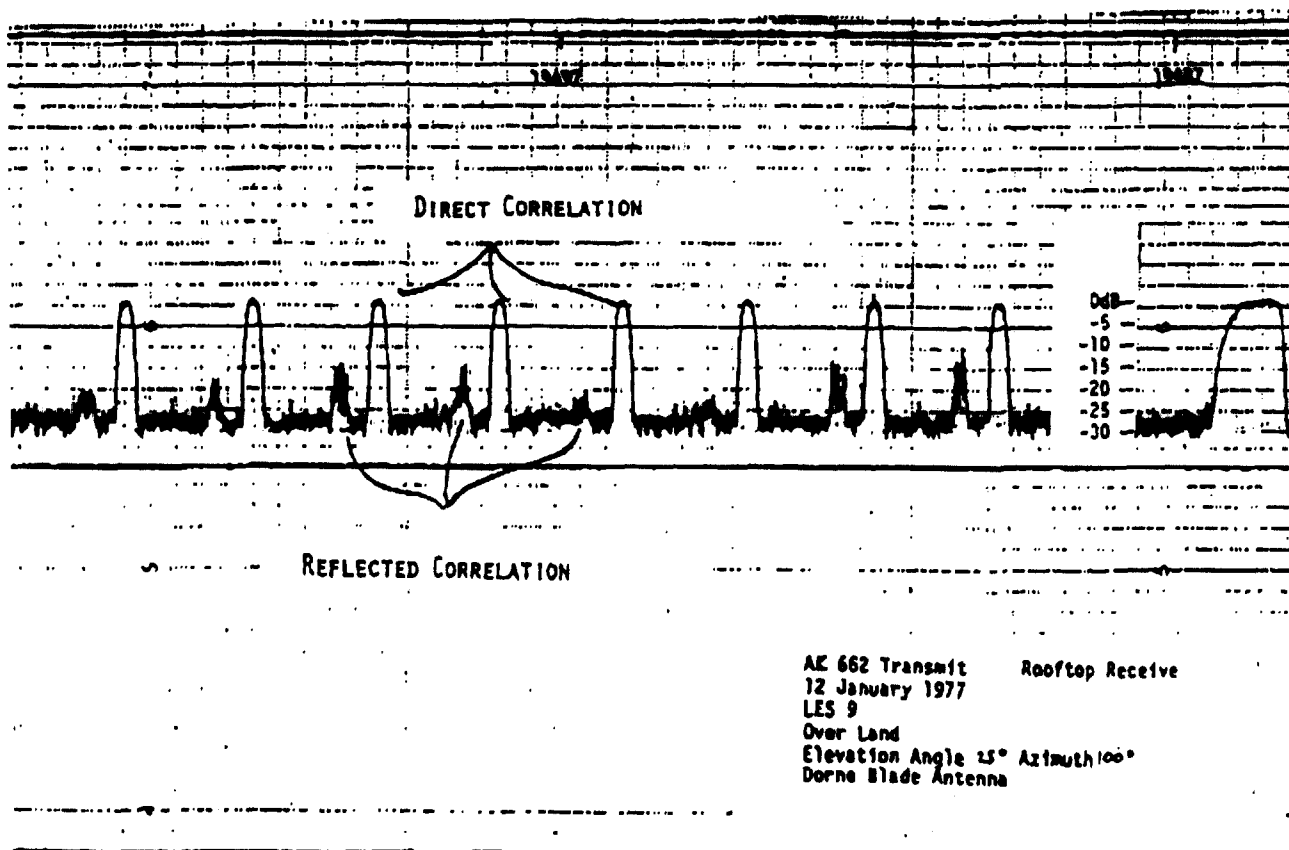


Fig.14 Results of PRN correlation with horizon antenna over land

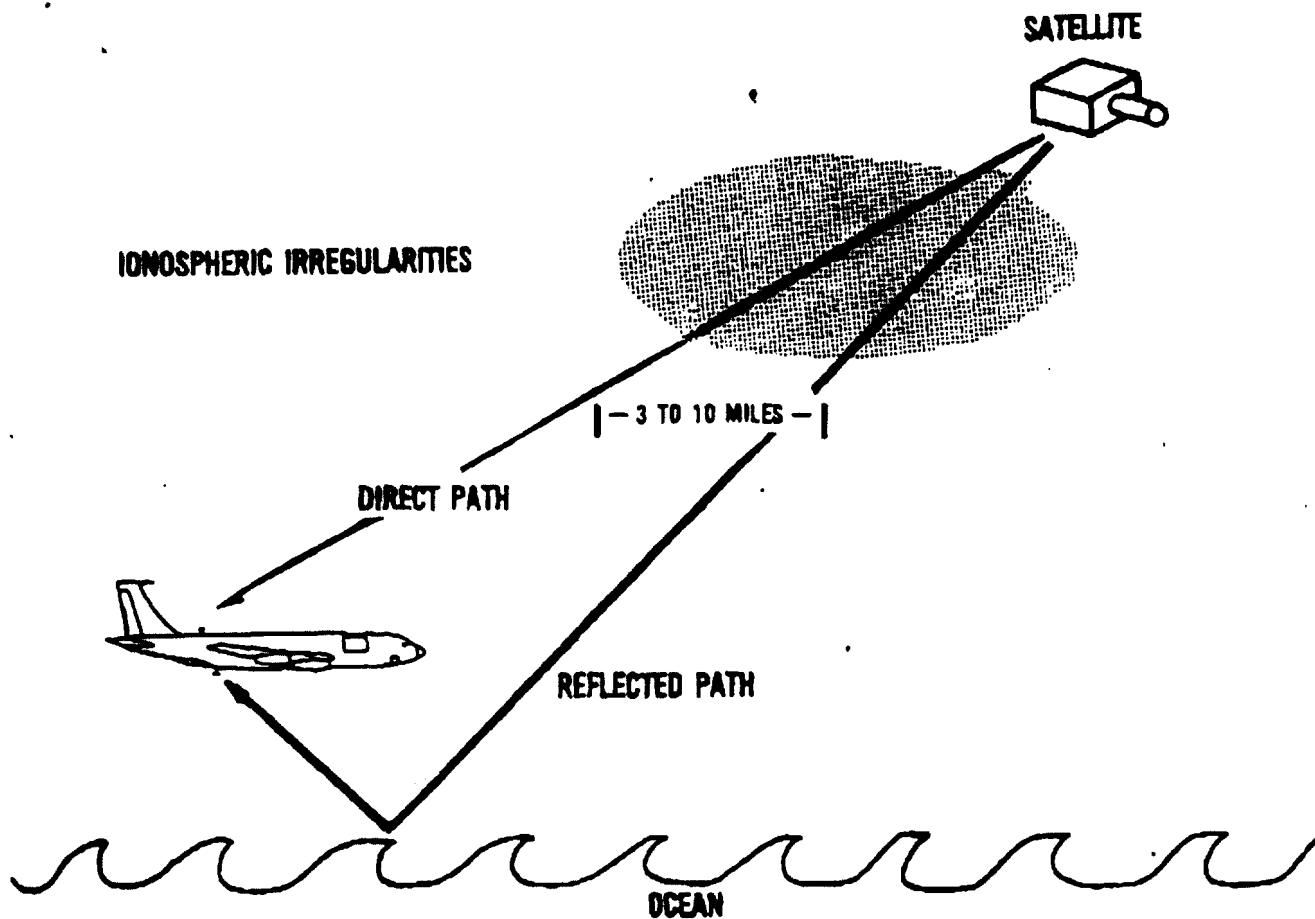


Fig.15 Geometry of fade mitigation technique

23 FEBRUARY 1979
 AIRCRAFT C-135/662
 LES 9 UHF CW TONE
 ELEVATION ANGLE 80°
 BOTTOM DORNE MARGOLIN
 CROSSED DIPOLE ANTENNA
 GULF of MEXICO

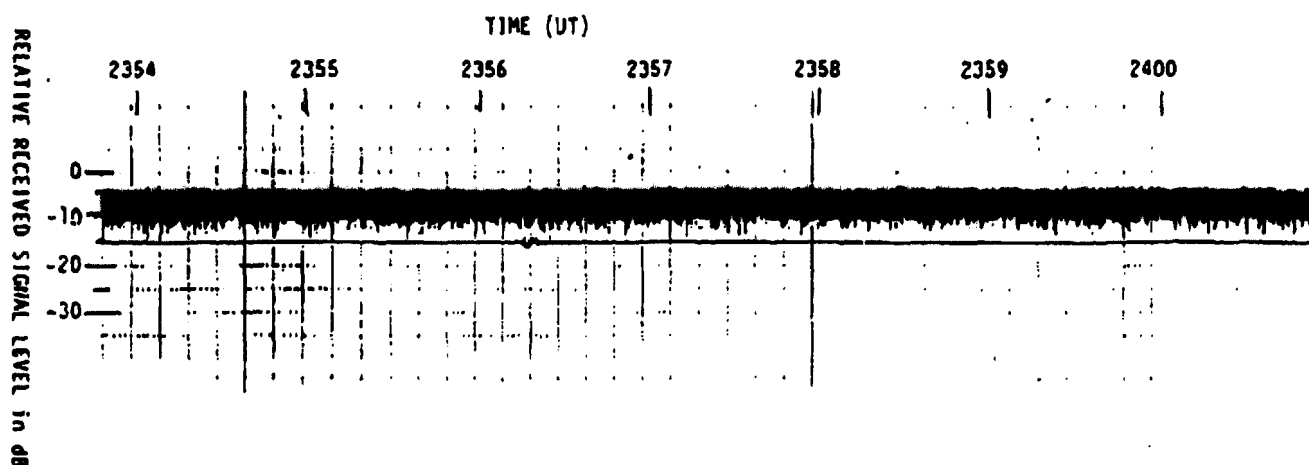


Fig.16 Received signal level from bottom antenna over water

23 FEBRUARY 1979
 AIRCRAFT C-135/662
 LES 9 UHF CW TONE
 BOTTOM DORNE MARGOLIN
 CROSSED DIPOLE ANTENNA
 ELEVATION ANGLE 80°
 TEXAS

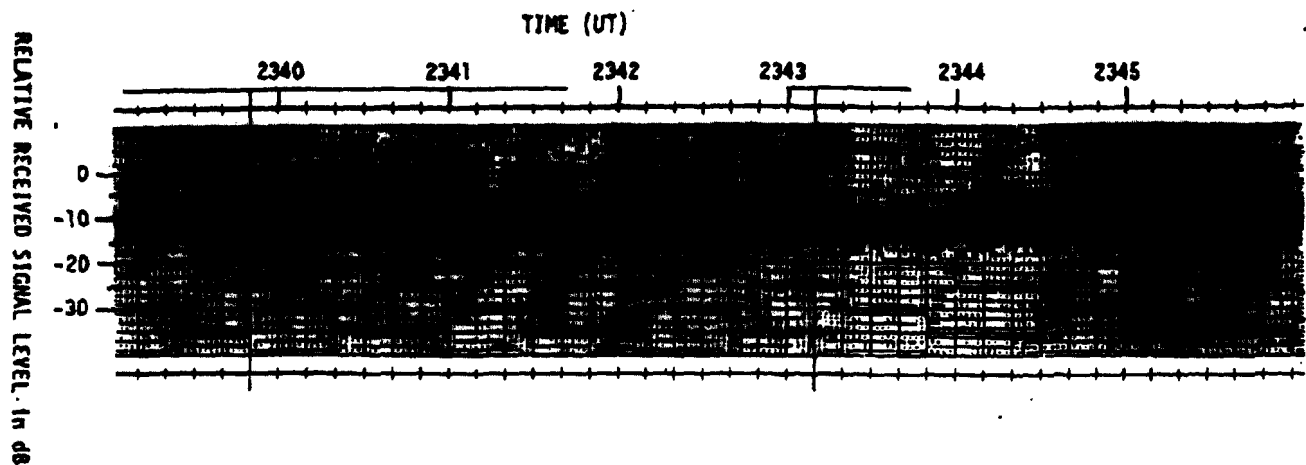


Fig.17 Received signal level from bottom antenna over land

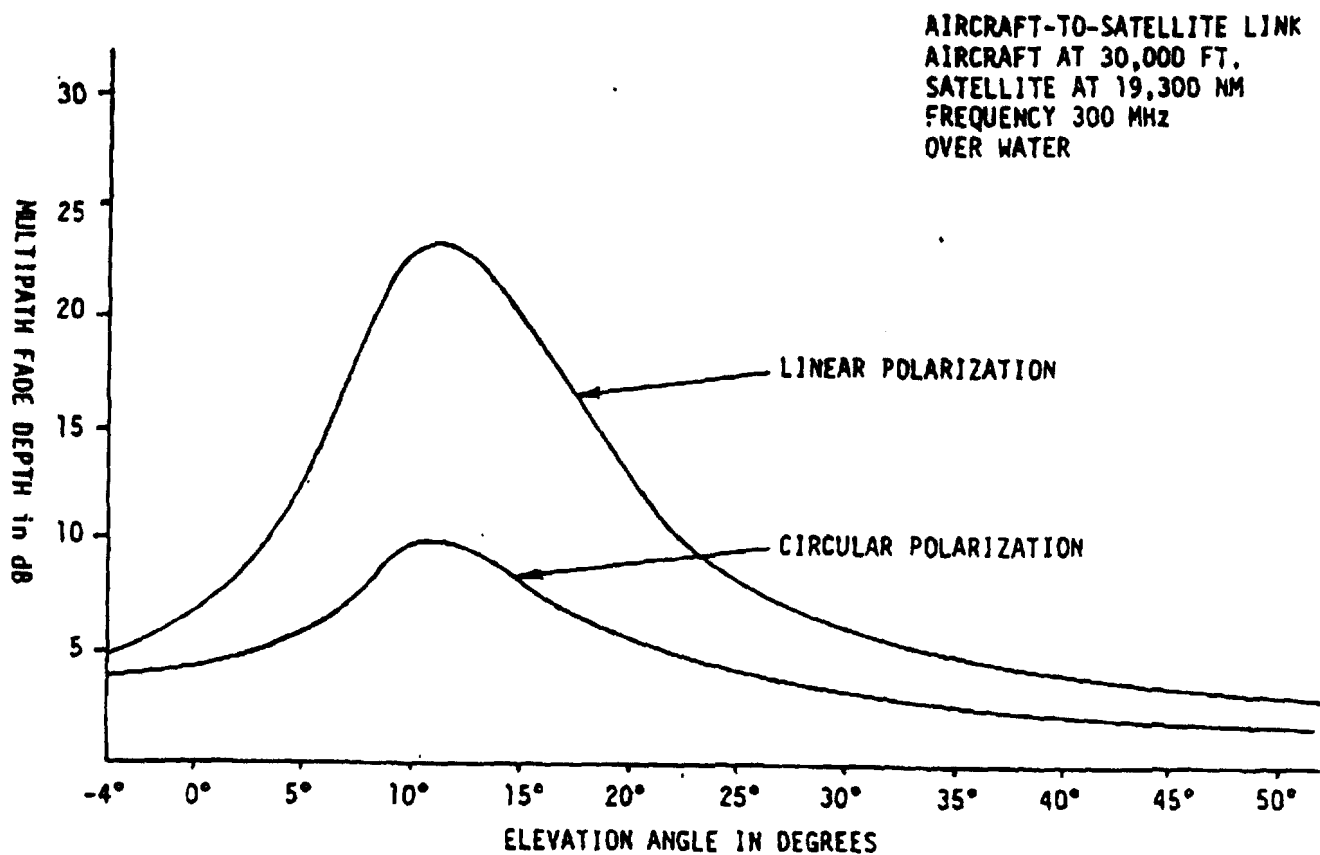


Fig.18 Typical multipath fading depth for linear and circular polarization

F_1

$F_2 = F_1 + 5\text{kHz}$

$F_3 = F_1 + 95\text{kHz}$

$F_4 = F_1 + 100\text{kHz}$

$F_5 = F_1 + 295\text{kHz}$

$F_6 = F_1 + 300\text{kHz}$

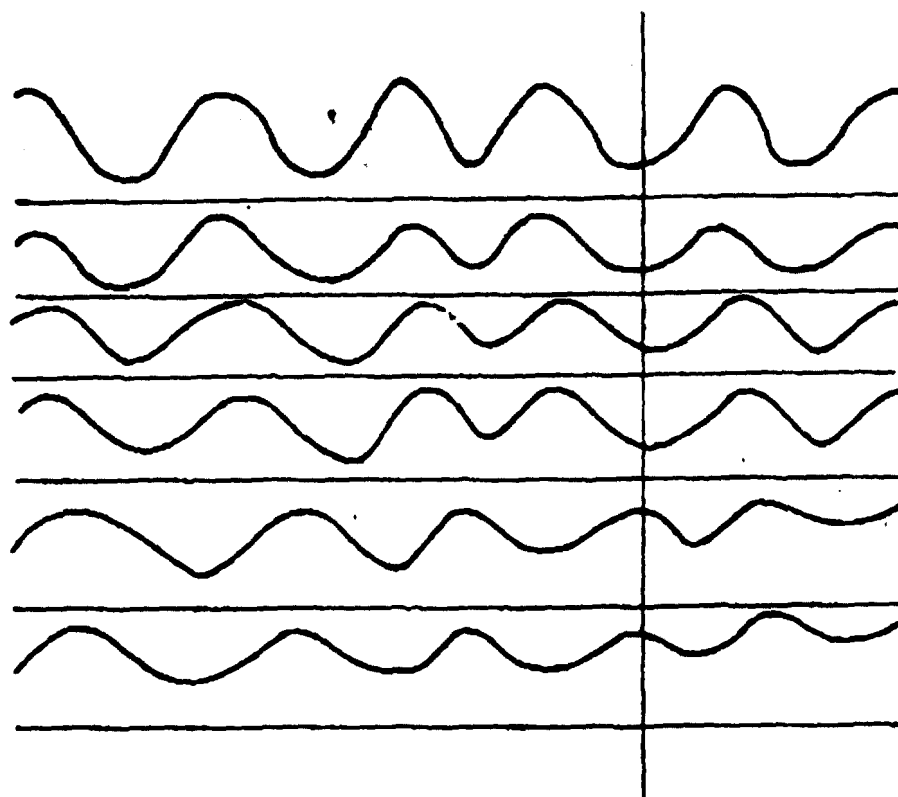


Fig.19 Multipath fading signal received over Greenland

16 JUNE 1977
AIRCRAFT C-135/662
LES 9 UHF
ELEVATION ANGLE 8°
TOP BLADE ANTENNA
POLAR CAP

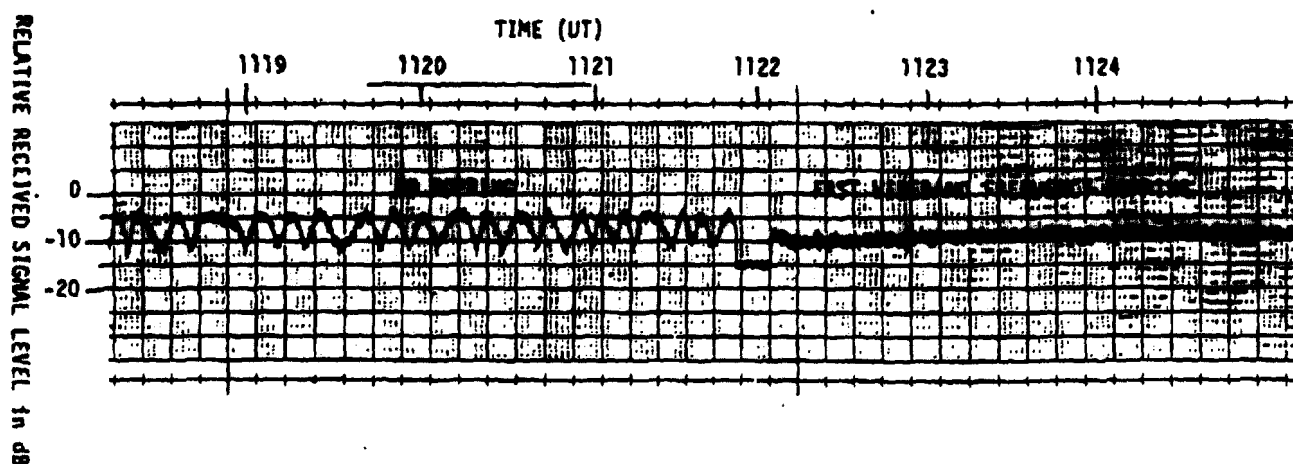


Fig.20 Multipath fading protection of fast frequency hopped signal

23 FEBURARY 1979
 AIRCRAFT C-135/662
 LES 9 UHF CW TONE
 ELEVATION ANGLE 81°
 BOTTOM DORNE MARGOLIN
 CROSSED DIPOLE ANTENNA
 TEXAS-GULF of MEXICO

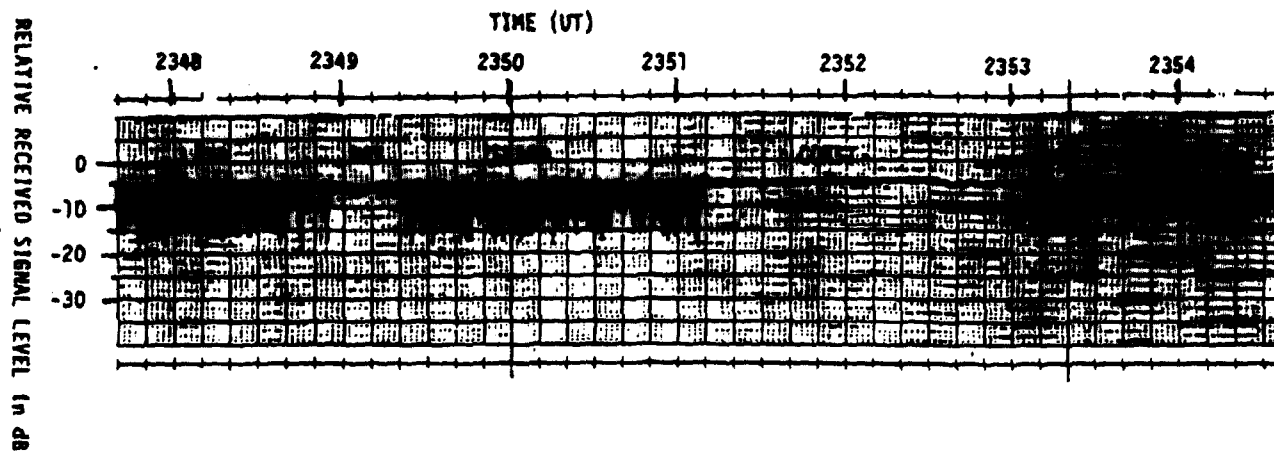


Fig.21 Coastal received signal level from bottom antenna

27 SEPTEMBER 1978
 AIRCRAFT C-135/662
 LES 8 UHF
 ELEVATION ANGLE 55°
 TOP DORNE MARGOLIN
 CROSSED DIPOLE ANTENNA
 GULF of MEXICO-LOUISIANA COAST

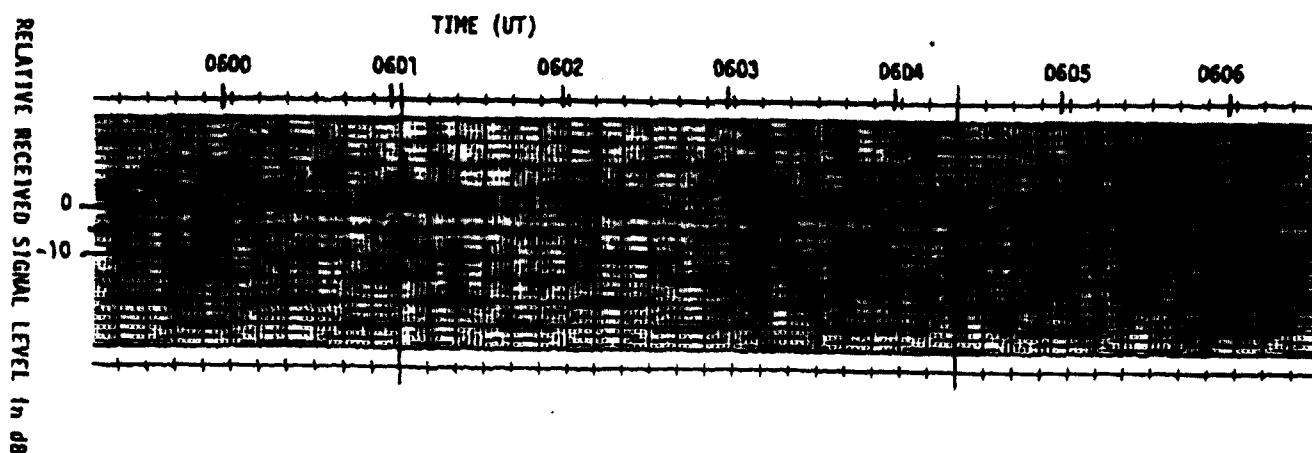


Fig.22 Coastal multipath fading received on top antenna